



Coleman–Weinberg inflation in light of Planck



Gabriela Barenboim^a, Eung Jin Chun^b, Hyun Min Lee^{c,*}

^a Departament de Física Teòrica and IFIC, Universitat de València–CSIC, E-46100, Burjassot, Spain

^b School of Physics, Korea Institute for Advanced Study, Seoul 130-722, Republic of Korea

^c Department of Physics, Chung-Ang University, Seoul 156-756, Republic of Korea

ARTICLE INFO

Article history:

Received 8 October 2013

Received in revised form 31 December 2013

Accepted 17 January 2014

Available online 23 January 2014

Editor: A. Ringwald

ABSTRACT

We revisit a single field inflationary model based on Coleman–Weinberg potentials. We show that in small field Coleman–Weinberg inflation, the observed amplitude of perturbations needs an extremely small quartic coupling of the inflaton, which might be a signature of radiative origin. However, the spectral index obtained in a standard cosmological scenario turns out to be outside the 2σ region of the Planck data. When a non-standard cosmological framework is invoked, such as brane-world cosmology in the Randall–Sundrum model, the spectral index can be made consistent with Planck data within 1σ , courtesy of the modification in the evolution of the Hubble parameter in such a scheme. We also show that the required inflaton quartic coupling as well as a phenomenologically viable $B - L$ symmetry breaking together with a natural electroweak symmetry breaking can arise dynamically in a generalized $B - L$ extension of the Standard Model where the full potential is assumed to vanish at a high scale.

© 2014 The Authors. Published by Elsevier B.V. Open access under [CC BY license](#). Funded by SCOAP³.

1. Introduction

The Hot Big-Bang Model and General Relativity successfully explain the thermal history of our Universe since its very first nanoseconds of existence up to now. However they left unexplained crucial issues such as the horizon, flatness, and monopole problems. Inflation is the most elegant and simple explanation to address them and therefore no modern cosmological model lacks a prudential stage of inflation. Inflation basically assumes the existence of a period of exponential growth of the scale factor which essentially wipes out any trace of curvature, dilutes unwanted relics and leaves the Universe in a highly symmetric state.

The simplest scenario where this picture can be realized is based on a single scalar field (called inflaton) with a nearly flat potential. The quantum fluctuations of the inflaton would be then responsible for the tiny temperature anisotropies observed in the Cosmic Microwave Background (CMB). Basically an inflationary theory must fulfill two requirements to agree with experimental observations: (i) it has to provide sufficient inflation, i.e., the inflationary potential must drive an increase on the scale factor of 50–60 e-folds (the precise number depends on details of the particular inflaton model) in order to describe the thermal equilibrium observed in the CMB at least for the scales of interest; (ii) the size of the quantum fluctuations of the inflaton leading to the power spectrum of primordial curvature perturbations, A_s , should be at

the appropriate level while the spectral index n_s must agree with observations. Because of these “mild” requirements most simple inflation models were given a death blow once the Planck mission released its high-precision data [1]. The Planck result, combined with the WMAP large-angle polarization measurements, requires the two observables n_s and A_s of curvature perturbations to be

$$n_s = 0.9603 \pm 0.0073, \quad A_s = 2.196^{+0.051}_{-0.060} \times 10^{-9} \quad (1)$$

at a scale $k_* = 0.05 \text{ Mpc}^{-1}$ which rules out exact scale-invariance at more than 5σ . Analogously, the tensor-to-scalar ratio r is bounded to be $r < 0.11$ at 95% CL, for the same scale k_* . These constraints are already powerful enough to rule out or strongly disfavor the most popular and simple inflationary potentials.

Consequently, simple and well motivated inflationary potentials are distinctively welcomed. Among these, a special place should be given to Coleman–Weinberg (CW) type of potentials [2] as they not only arise naturally but are unavoidable when loop corrections are taken into account. Inflation with a CW potential has been suggested at an early stage of the inflation theory formulation, and studied extensively, in particular, in association with grand unification theories [3].

In this Letter, we revisit the CW inflation accounting for cosmological observations in a scheme where the inflaton potential has a dynamical origin, naturally arising from quantum corrections. As we will see later, the quartic coupling of the CW potential is proportional to the amplitude of primordial perturbations and thus has to be extremely small ($\sim 10^{-14}$) which might point towards

* Corresponding author.

a radiative origin. An attempt to generate a phenomenologically viable scalar potential starting from a vanishing initial condition of the full scalar potential at a cutoff scale has been worked out in the context of the $SU(3)_c \times SU(2)_L \times U(1)_Y \times U(1)_X$ model where $U(1)_X$ is a generalized $B - L$ gauge symmetry [4]. It has been shown that a Standard Model (SM) Higgs potential consistent with recent LHC data [5] can be generated radiatively once the $B - L$ symmetry is broken appropriately by the usual CW mechanism. One of the distinctive features of this scheme is that the quartic coupling of the $B - L$ scalar arises due to its coupling to right-handed neutrinos in a similar way as the SM scalar quartic coupling arises due to the top Yukawa coupling.

We find that in a general CW inflation model, the number of e-folding required for solving the horizon problem cannot be made consistent with the observed spectral index. That is, the spectral index resulting from getting enough number of e-folds to take care of the horizon problem, can only fit within the 3σ range of the Planck data for a symmetry breaking scale larger than 10^{15} GeV. In particular, when using a value of the symmetry breaking scale favored for providing natural electroweak symmetry breaking in a generalized $B - L$ extension of the SM, the resulting spectral index is well outside the 5σ range of the Planck data. This motivates us to consider the CW inflation in a non-standard cosmological scenario, a typical example of which is brane cosmology in a higher dimensional space such as the Randall–Sundrum model [6,7]. In this case, the extra dimension does not evolve in time while the evolution of 4-dimensional spacetime is described by a modified Friedman equation, where $H^2 \propto \rho^2$ in the large energy density limit. Thus, the effective inflaton energy increases by a factor, V_0/Λ , with V_0 being the original inflaton energy and Λ being the brane tension, which makes the CW inflation fully compatible with the observations for an appropriate choice of the brane tension. A remarkable feature of the CW inflation on the brane is that the correlations between the observables are kept the same as in the standard CW inflation.

The Letter is organized as follows. We begin by revisiting CW inflation in standard cosmology in Section 2. In Section 3 the setup is extended to brane cosmology and the inflationary observables are calculated for the modified Friedman equation. We show in Section 4 how the required quartic coupling and symmetry breaking scale for the CW inflaton potential can be generated in the context of the $B - L$ extension of the SM which is motivated by the explanation of the neutrino masses and mixing. Finally, conclusions are drawn in Section 5.

2. CW inflation in standard cosmology

A general CW potential evaluated at the renormalization scale $Q = \langle\phi\rangle = v_\phi$ takes a rather simple form:

$$V(\phi) = A\phi^4 \left(\log\left(\frac{\phi}{v_\phi}\right) - \frac{1}{4} \right) + \frac{A}{4} v_\phi^4 \quad (2)$$

which satisfies $V'(v_\phi) = 0$ and $V(v_\phi) = 0$. Here $A = A(v_\phi)$ is determined by the beta function for the scalar quartic coupling defined at $Q = v_\phi$, which is a function of gauge, Yukawa and other scalar couplings of the inflaton field ϕ . A detailed form of the beta function and the CW potential applied to the $B - L$ gauge symmetry will be discussed later. Depending on the values of A and v_ϕ , the inflaton can have small or large values compared to the Planck scale during observable inflation. In the latter case inflation mimics chaotic inflation. We will be interested in the scenario where the inflaton starts its journey from small values of the field, $\phi/v_\phi < 1$, in the flat region of the CW potential as drawn in Fig. 1. There is a

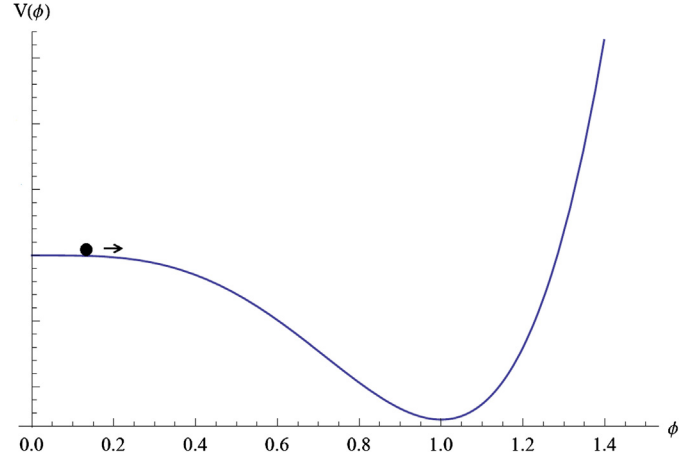


Fig. 1. The CW potential realizing a small field inflation.

recent overview on various inflation models including the CW type inflation [8].

During inflation, the inflaton rolls down towards the minimum of its potential, evolving according to

$$\ddot{\phi} + 3H\dot{\phi} + \partial V/\partial\phi = 0 \quad (3)$$

where the Hubble rate H is given by

$$H^2 = \frac{1}{3M_p^2} \left[\frac{\dot{\phi}^2}{2} + V(\phi) \right]. \quad (4)$$

Here $M_p \approx 2.44 \times 10^{18}$ GeV is the reduced Planck mass. If the field is moving along a region where the potential is so flat that the evolution of the field is friction dominated (what goes in the literature under the name of slow-roll approximation), the equation of motion is basically given by

$$3H\dot{\phi} + \partial V/\partial\phi \approx 0. \quad (5)$$

Within this approximation, the number of e-folds of inflation generated since the modes that are entering the observable Universe now left the horizon (at ϕ_*) till the end of inflation (at ϕ_f) is given by

$$N(\phi_*) = -\frac{1}{M_p^2} \int_{\phi_*}^{\phi_f} \frac{V(\phi)}{V'(\phi)} d\phi \quad (6)$$

where $V'(\phi) = \partial V/\partial\phi$ and ϕ_f is the value of the field at which inflation stops. This happens when

$$\epsilon(\phi_f) \equiv \frac{M_p^2}{2} \left[\frac{V'(\phi_f)}{V(\phi_f)} \right]^2 = 1. \quad (7)$$

At this time, quantum fluctuations on the scale observed today were produced too and its size is given by

$$\mathcal{P}_{\mathcal{R}}(k_*) = \frac{1}{24\pi^2} \frac{V(\phi_*)}{M_p^4 \epsilon(\phi_*)} \quad (8)$$

while the spectral index of these density perturbations and its dependence on the scale read

$$n_s - 1 = -6\epsilon(\phi_*) + 2\eta(\phi_*), \quad (9)$$

$$\frac{dn_s}{d \ln k} = 16\epsilon(\phi_*)\eta(\phi_*) - 24\epsilon(\phi_*)^2 - 2\xi^2(\phi_*). \quad (10)$$

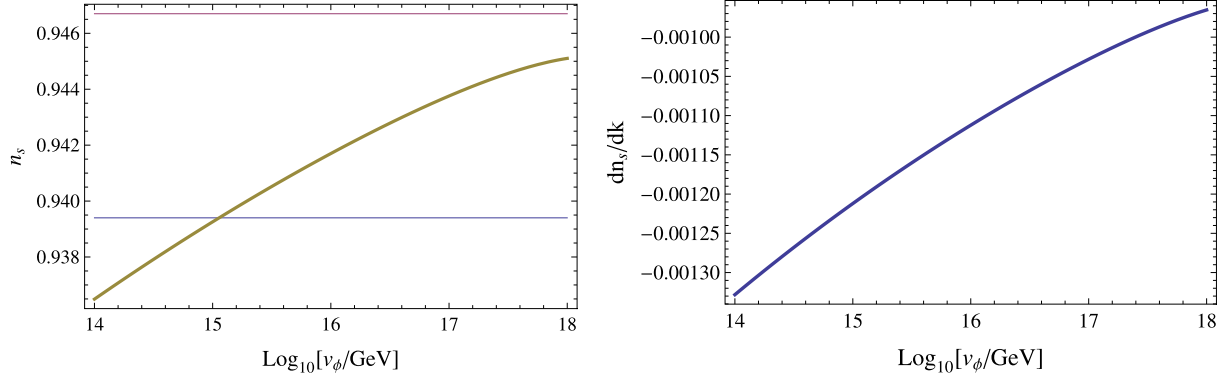


Fig. 2. The spectral index n_s and its running as a function of v_ϕ in the standard CW inflation. Two horizontal lines in the left panel show 2σ and 3σ lower bounds measured by Planck, respectively.

Here, η and ξ^2 are the second and third slow-roll parameters that can be expressed in terms of the inflaton potential as

$$\eta = M_P^2 \frac{V''}{V} \quad \text{and} \quad \xi^2 = M_P^4 \frac{V'''V'}{V^2}. \quad (11)$$

Besides the observed density (scalar) perturbations, the inflaton generates the yet unobserved gravitational waves or tensor perturbations. Normally, the tensor amplitude is expressed in terms of the tensor/scalar ratio as

$$r \equiv \frac{\mathcal{P}_T}{\mathcal{P}_R} = 16\epsilon(\phi_*). \quad (12)$$

Expressed in terms of the parameters of the CW potential (2), the above inflation quantities are given explicitly by

$$\epsilon = 8 \left(\frac{4M_P}{v_\phi} \right)^2 \left(\frac{\phi}{v_\phi} \right)^6 \ln^2 \left(\frac{\phi}{v_\phi} \right), \quad (13)$$

$$\eta = \left(\frac{4M_P}{v_\phi} \right)^2 \left(\frac{\phi}{v_\phi} \right)^2 \left(3 \ln \left(\frac{\phi}{v_\phi} \right) + 1 \right), \quad (14)$$

$$\xi^2 = \left(\frac{4M_P}{v_\phi} \right)^4 \left(\frac{\phi}{v_\phi} \right)^4 \ln \left(\frac{\phi}{v_\phi} \right) \left(6 \ln \left(\frac{\phi}{v_\phi} \right) + 5 \right), \quad (15)$$

$$N = \left(\frac{v_\phi}{4M_P} \right)^2 \left(\text{Ei} \left[-2 \ln \left(\frac{\phi}{v_\phi} \right) \right] - \text{Ei} \left[-2 \ln \left(\frac{\phi_f}{v_\phi} \right) \right] \right), \quad (16)$$

$$\mathcal{P}_R(k) = \frac{A}{3\pi^2} \left(\frac{v_\phi}{4M_P} \right)^6 \left(\frac{v_\phi}{\phi} \right)^6 \frac{1}{\ln^2 \left(\frac{\phi}{v_\phi} \right)}, \quad (17)$$

where Ei stands for the exponential integral.

From the equations above, one can see that for slow-roll inflation to take place, a field value ϕ_* at horizon exit can be always found for *any* choice of v_ϕ and it lays in the region of $\phi_*/v_\phi \ll 1$ as the slow-roll parameters have a large factor of $(4M_P/v_\phi)^2$. This leads to $|\epsilon| \ll |\eta| \approx \sqrt{3}|\xi^2|/2$. As a consequence, small field CW inflation predicts remarkable correlations:

$$N \approx \frac{3}{1 - n_s}, \quad (18)$$

$$\frac{dn_s}{d \ln k} \approx -\frac{1}{3}(1 - n_s)^2, \quad (19)$$

independently of the precise values of v_ϕ and ϕ/v_ϕ . Similarly, the power spectrum of perturbation is

$$\mathcal{P}_R(k) \approx A \frac{72}{\pi^2} \frac{|\ln(\phi/v_\phi)|}{(1 - n_s)^3}, \quad (20)$$

which is insensitive to ϕ/v_ϕ . Considering the central value of $n_s = 0.96$ and $\mathcal{P}_R \approx 2.2 \times 10^{-9}$ measured by the Planck mission at the pivot scale $k_* = 0.05 \text{ Mpc}^{-1}$ [1], one gets $N \approx 75$, and $A \sim 10^{-14}$ mildly depending on ϕ_* . The tensor-to-scalar ratio given by

$$r \approx \frac{16}{27} \left(\frac{v_\phi}{4M_P} \right)^4 \frac{(1 - n_s)^3}{|\ln(\phi/v_\phi)|} \quad (21)$$

is severely suppressed by a factor of $(v_\phi/M_P)^4$ while being insensitive to ϕ .

Such large N and tiny A do not fit well with the number of e-folding required to solve the horizon problem for scales that have just entered/are entering the current horizon. The condition for such a thing to happen is

$$1 = \frac{(aH)_*}{(aH)_0} = \frac{a_*}{a_{\text{end}}} \cdot \frac{a_{\text{end}}}{a_{\text{reh}}} \cdot \frac{a_{\text{reh}}}{a_0} \cdot \frac{H_*}{H_0}, \quad (22)$$

which translates into

$$\begin{aligned} N_* &= \frac{1}{3} \ln \left(\frac{\rho_{\text{reh}}}{\rho_{\text{end}}} \right) + \frac{1}{4} \ln \left(\frac{\rho_{0r}}{\rho_{\text{reh}}} \right) + \frac{1}{2} \ln \left(\frac{\rho_*}{\rho_0} \right) \\ &\simeq 61 - \ln \left(\frac{10^{16} \text{ GeV}}{V_*^{1/4}} \right) + \ln \left(\frac{V_*^{1/4}}{V_{\text{end}}^{1/4}} \right) - \frac{1}{3} \ln \left(\frac{V_{\text{end}}^{1/4}}{\rho_{\text{reh}}^{1/4}} \right) \end{aligned} \quad (23)$$

where $\rho_{0(r)}$, ρ_{reh} , ρ_{end} are (radiation) energy densities at present, the end of reheating and the end of inflation, respectively, and ρ_* , V_* are energy density and inflaton potential evaluated at horizon exit for the pivot scale $k_* = 0.05 \text{ Mpc}^{-1}$. Note that one can take $V_* \simeq V(0) \simeq V_{\text{end}}$ as a good approximation in most cases. For the CW picture of inflation to work, the number of e-folds $N|_{\phi_*}$ (16) derived from the CW potential should be able to reproduce the number N_* (23). This condition together with the COBE normalization, $\mathcal{P}_R \simeq 2.2 \times 10^{-9}$, and the CW inflation property, $n_s \simeq 1 + 2\eta$, uniquely fixes the values of the three parameters, A , v_ϕ and ϕ/v_ϕ of the CW potential.

The obtained spectral index n_s for a given symmetry breaking scale v_ϕ is shown in Fig. 2. The largest possible value that n_s can take is about 0.945 for v_ϕ close to M_P which is below the 2σ range favored by the Planck data. Only a 3σ compatibility can be achieved for $v_\phi \gtrsim 10^{15} \text{ GeV}$, disfavoring CW inflation at the 2σ level. The running of the spectral index is presented in the right panel of Fig. 2 which shows a strong correlation between the spectral index and its running as discussed before. The obtained running has to be compared with Planck's result

$$\frac{dn_s}{d \ln k} = -0.013 \pm 0.009 \quad (24)$$

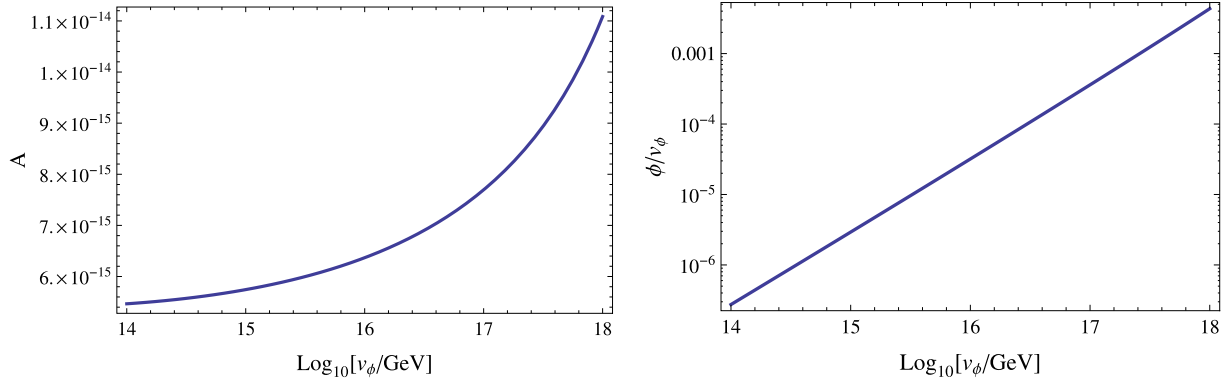


Fig. 3. The correlations of A and ϕ/v_ϕ with v_ϕ for the CW inflation in the standard cosmology.

at 68% CL. It is clear that the results have no definite impact on this class of models, but they are bounded to test them in the near future as the precision on both measurements, the spectral index and its running will be significantly improved.

In Fig. 3, we present the values of A and ϕ/v_ϕ for given v_ϕ showing a correlation between A and ϕ/v_ϕ . One finds that smaller v_ϕ require smaller A and ϕ/v_ϕ , but one gets $A \sim 10^{-14}$ which is rather insensitive to v_ϕ . As mentioned earlier, we find $\phi/v_\phi \ll 1$ for all the region of $v_\phi < M_P$.

The strong tension of the CW inflationary setup with Planck data arises due to the fact that V_* cannot be made large enough to enhance N_* as a tiny quartic coupling A is also required by the size of perturbations, and even though one can have v_ϕ as large as M_P it is not enough to overcome the strong A suppression. The tension is aggravated even further if one wants to have lower symmetry breaking scales in the CW mechanism. This problem may be avoided in a non-standard cosmological scenario where the relation (23) is altered in a radical way. Most of the modifications we can get within the standard framework, like an earlier period of matter domination, work in the opposite direction, i.e. they lower the number of e-folding needed to solve the horizon problem.

3. CW inflation on the brane

For a drastic change in the thermal history of the Universe we can immerse ourselves into a brane world scenario where we live in a brane embedded in a higher dimensional Universe. Within this scheme, the stress-energy momentum in the bulk can take different forms, depending on the specifics of the model. By an appropriate choice of the boundary conditions, the non-standard behavior of the Universe on the brane we are looking for, can be easily achieved. Even more, the Hubble rate itself on the brane changes rather drastically taking the form

$$H^2 = \frac{1}{3M_P^2} \rho \left(1 + \frac{\rho^n}{M_B^{4n}} \right) + \frac{C}{a^4} \quad (25)$$

where M_B denotes a certain scale below which the cosmological evolution follows the standard form. A useful model to illustrate these effects is the brane world cosmology of the Randall-Sundrum (RS) model [7] in which the main correction is the term quadratic in the density, i.e.,

$$H^2 = \frac{1}{3M_P^2} \rho \left(1 + \frac{\rho}{2\Lambda} \right), \quad (26)$$

and the new scale M_B is given by the brane tension $\Lambda = M_B^4/2$ satisfying $\Lambda = \sqrt{-6\Lambda_{\text{bulk}} M_5^3}$ where Λ_{bulk} is the bulk cosmological constant and M_5 is the 5-dimensional Planck scale [6].

During the inflationary stage the energy momentum tensor on the brane is dominated by the scalar field, which is confined to it and therefore still evolves as Eq. (3), as on the brane $\nabla^\nu T_{\mu\nu} = 0$ holds. The condition to sustain a period of inflation is now

$$p < -2/3\rho \quad (27)$$

for $\rho \gg \Lambda$ and when the energy density is dominated by the scalar potential

$$H^2 \simeq \left(\frac{1}{3M_P^2} \right) V \left[1 + \frac{V}{2\Lambda} \right]. \quad (28)$$

In this regime the slow-roll parameters become

$$\epsilon_B = \epsilon \cdot \frac{1 + 2\tilde{V}}{(1 + \tilde{V})^2}, \quad (29)$$

$$\eta_B = \eta \cdot \frac{1}{1 + \tilde{V}}, \quad (30)$$

$$\xi_B^2 = \xi^2 \cdot \frac{1}{(1 + \tilde{V})^2}, \quad (31)$$

where we have defined $\tilde{V} \equiv V/M_B^4$.

Note that all the slow-roll parameters recover their standard forms for $\tilde{V} = 0$, but are suppressed by $1/\tilde{V}$ in the limit of $\tilde{V} \gg 1$. While the spectral index takes the same form: $n_s = 1 - 6\epsilon_B + 2\eta_B$, its running is given by

$$\frac{dn_s}{d \ln k} = -2\xi_B^2 + 16\epsilon_B\eta_B - 24\epsilon_B^2 \cdot \frac{1 + 3\tilde{V} + 3\tilde{V}^2}{(1 + 2\tilde{V})^2}. \quad (32)$$

The power spectrum of primordial quantum fluctuations and the tensor-to-scalar ratios are also modified to turn into

$$\mathcal{P}_{\mathcal{R},B}(k) = \mathcal{P}_{\mathcal{R}}(k) \cdot (1 + \tilde{V})^3, \quad (33)$$

$$r_B = 16\epsilon_B \frac{1}{1 + 2\tilde{V}}. \quad (34)$$

The number of e-folding during inflation is also changed to

$$N_B = -\frac{1}{M_P^2} \int_{\phi_*}^{\phi_f} \frac{V}{V'} (1 + \tilde{V}) d\phi. \quad (35)$$

The condition for solving the horizon problem now gets an extra term which leads to an additional number of e-folding for the scales of interest ($k_* = 0.05 \text{ Mpc}^{-1}$) depending on \tilde{V} :

$$N_{B,*} \approx 61 + \frac{1}{2} \ln(1 + \tilde{V}) - \ln \left(\frac{10^{16} \text{ GeV}}{V_*^{1/4}} \right) - \frac{1}{3} \left(\frac{V_*^{1/4}}{\rho_{\text{reh}}^{1/4}} \right). \quad (36)$$

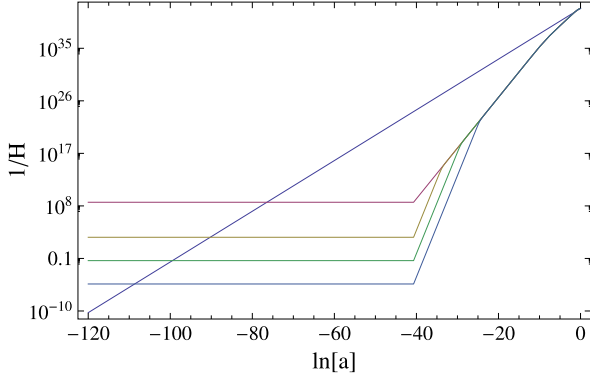


Fig. 4. Evolution of the horizon size in a brane cosmology with $n = 1$ and $V_*^{1/4} = 10^5$ GeV in terms of $\ln(a)$ with the normalization of $a_{\text{now}} = 1$. The four lines correspond to $M_B = \infty$ (standard), 10^2 , 1 and 10^{-2} GeV from the top, respectively, showing how the e-folding number after the horizon exit of the current horizon scale changes.

This increase can be easily understood by seeing in Fig. 4 how steeper the Hubble radius change is, once the new scenario kicks in. The lower the scale associated with the new scenario (the brane tension) the larger the required number of e-folds for a fixed value of the potential at the end of inflation, i.e., for a fixed reheating temperature or a fixed scale factor for the end of inflation. From the figure, it is immediate to see how the number of e-folds required to solve the horizon problem (basically the number of e-folds evolved by our Universe since reheating) changes for the current horizon scale depending on the brane scenario scale M_B . For this figure, we have taken a low inflation scale $V_*^{1/4} = 10^5$ GeV and the end of inflation to happen at $\ln(a) \approx -40$. Note that the commonly used value of $N \approx 60$ is obtained for $M_B = 1$ GeV.

Before continuing the numerical analysis of the CW brane inflation, we briefly discuss the consistency of introducing a huge change with $\tilde{V} = V/(2\Lambda) \gg 1$ in the Friedman equation. First, we note that the length scale on the brane is determined by $L \sim |R_{\mu\nu\alpha\beta}|^{-1/2} \sim |T_{\mu\nu}/M_P^2|^{-1/2} \sim V^{-1/2} M_P$. On the other hand, the length scale in the bulk is related to the AdS length scale, $l \sim \Lambda^{-1/2} M_P$, due to the relations to the input parameters in the RS model, $l = \sqrt{6M_5^3/|\Lambda_{\text{bulk}}|}$ and $\Lambda = \sqrt{6M_5^3|\Lambda_{\text{bulk}}|}$ with $M_P^2 \sim M_5^3 l$. Thus, taking $V/(2\Lambda) \gg 1$, we are in the regime that $L/l \sim (\Lambda/V)^{1/2} \ll 1$ where the continuum of KK modes in the RS II model with a single brane could be easily excited during inflation and affect the slow-roll inflation on the brane. Therefore, we need to stabilize the radius of extra dimension, for instance, by introducing a second brane in the bulk, so that the KK modes become discrete and decoupled during inflation. We don't go to the details on the radius stabilization in our work and we just assume that a radius stabilization mechanism of Goldberger–Wise type [9] is at work. Then, the radius should be stabilized at a small value such that the KK masses are larger than the Hubble parameter during inflation. Moreover, in order for the inflaton potential not to destabilize the radius, the mass of the radion, namely, the excitation of the radius, must also satisfy $m_r^2 \gtrsim H^2$ where $H^2 \sim \tilde{V}_* V_*/M_P^2$. For instance, for $V_*^{1/4} = 10^5$ GeV and $\Lambda^{1/4} = M_B = 1$ GeV, we get $\tilde{V}_* \sim 10^{20}$ so the radion mass should be $m_r \gtrsim 100$ GeV. Consequently, we can accommodate in our setup a light radion relevant for collider physics and still be compatible with inflationary phenomenology contrary to the high-scale case.

Let us now examine how successful inflationary solutions satisfying the conditions, $\mathcal{P}_{\mathcal{R},B}(k_*) = 2.2 \times 10^{-9}$ and $N_B = N_{B,*}$, can arise in the limit of $\tilde{V} \gg 1$. For given v_ϕ and M_B , these conditions can be solved uniquely by appropriate values of A and ϕ/v_ϕ as

shown in Figs. 5 (varying M_B) and 6 (varying v_ϕ) for high and low v_ϕ (M_B), respectively.

When M_B is not so small that the ϕ -independent prefactor of the modified slow-roll parameters (e.g., $\eta_B \approx \eta/\tilde{V}$) remains much larger than one: $(4M_P/v_\phi)^2(4M_B^4/Av_\phi^4) \gg 1$, one still finds solutions for $\phi/v_\phi \ll 1$ leading to $|\epsilon_B| \ll |\eta_B| \approx \sqrt{2|\xi_B^2|/3}$ as in the standard cosmology. Thus, the simple correlations in Eqs. (18), (19), (20) still hold. This behavior can be seen from the solution lines corresponding to the large region of M_B and the small region of v_ϕ in each panel of Figs. 5 and 6, respectively. As M_B (v_ϕ) becomes smaller (larger) starting from the right (left) end in Fig. 5 (6), the CW parameters, ϕ/v_ϕ and A , as well as the inflationary observables, n_s and dn_s/dk , increase monotonically, and n_s reaches its local maximum at around 0.946 corresponding to $\phi/v_\phi \sim 0.01$. This is the exactly same pattern as in Figs. 2 and 3 where the four quantities increase as v_ϕ gets close to M_P , and $n_s(\phi/v_\phi)$ approaches 0.945 (0.01) maximally allowed in the region of $v_\phi < M_P$. One can also check that the relation (19) holds intact in this small ϕ/v_ϕ region. Note that the spectral can be enhanced a lot even for low v_ϕ (Fig. 6) by choosing appropriate M_B , but is still limited below the Planck's 2σ lowest value in the region of $\phi/v_\phi \lesssim 0.01$ as in the standard cosmology.

When M_B (v_ϕ) becomes even smaller (larger) in Fig. 5 (6), one finds solutions with $\phi/v_\phi \gtrsim 0.01$ eventually approaching the one for which the standard relations (18), (19), (20) are invalidated, but new correlations appear. The spectral index (and also its running) starts to rise rapidly at $\phi/v_\phi \sim 0.1$, but it reaches its maximum value ~ 0.966 (-0.005) and then decreases slowly to approach 0.96 (-0.006). In this large ϕ/v_ϕ region, the spectral index (and its running) is dominated by the ϵ_B contribution. One can see that there appears a new correlation between these two observables, which is different from the standard one (19). Note that A becomes much smaller than the typical value $\sim 10^{-14}$ in the asymptotic region preventing the prefactor $(4M_P/v_\phi)^2(4M_B^4/Av_\phi^4)$ becoming too small and thus allowing solutions with ϕ/v_ϕ close to one.

Let us remark that the four lines in each panel of Figs. 5 and 6 show the same behavior as functions of ϕ/v_ϕ , that is, one can always find an appropriate range of M_B and v_ϕ reproducing the same values of n_s and dn_s/dk , as well as the same correlation between them. Of course, M_B cannot be taken to be smaller than $O(1)$ MeV for which the standard big-bang nucleosynthesis prediction is spoiled. We find that a spectral index within 1σ range of the Planck data can be obtained for $v_\phi \gtrsim 3 \times 10^7$ GeV with the restriction of $M_B > 10$ MeV. As in the standard cosmology, there is also a remarkable correlation between the running of the spectral index and the spectral index itself. Taking the 1σ range of the Planck data for the spectral index, $n_s = (0.9540, 0.9686)$, the CW inflation on the brane predicts

$$\frac{dn_s}{d \ln k} = (-0.00064, -0.0005). \quad (37)$$

It is worth noticing that this kind of correlation is unique to CW potentials and cannot be avoided and therefore provides a crucial test on the model. The ratio of tensor to scalar perturbations is not shown because although it is different from zero and negative, its actual value is so tiny that it is effectively zero from an experimental point of view. Again this feature cannot be circumvented in the CW inflation, and therefore the measurement of gravity waves will completely rule out small-field CW inflation.

The allowed ranges of the symmetry breaking scale, $v_\phi \sim 10^8$ GeV, and the quartic coupling, $A \sim 10^{-14}$, shown in Fig. 6, are of our special interest as such small values of A can have a dynamical origin in a model where the full scalar potential, including

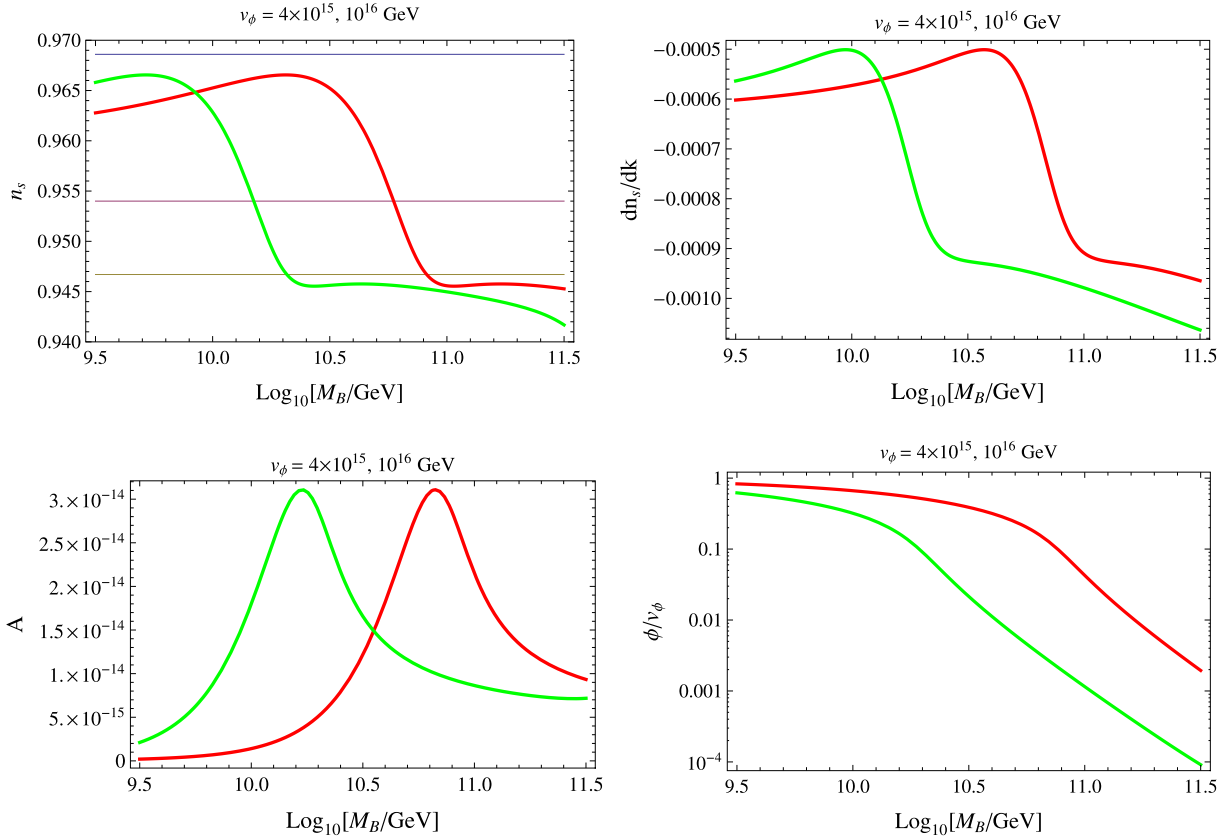


Fig. 5. The spectral index n_s , its running dn_s/dk , the quartic coupling A and the horizon-exit field value of ϕ/v_ϕ are shown in terms of the brane scale M_B for fixed symmetry breaking scales $v_\phi = 4 \times 10^{15}$ GeV (left green curve) and 10^{16} GeV (right red curve) in each panel. The upper two horizontal lines in the first panel show n_s within the 1σ range of the Planck data and the lower line is the 2σ limit. (For interpretation of the references to color in this figure legend, the reader is referred to the web version of this Letter.)

both the inflaton and Higgs sectors, can be generated purely from radiative corrections.

4. Dynamical generation of the inflaton potential

As a specific example of the CW inflation, let us consider the SM extended with a generalized $U(1)_{B-L}$ gauge symmetry. In its minimal setup where the $U(1)$ charges are given by a linear combination of $B-L$ charge and hypercharge as $X = Y_{B-L} - xY$, the model requires three right-handed neutrinos which couple to a $B-L$ Higgs field Φ and thus acquire heavy Majorana masses after the $B-L$ symmetry breaking:

$$\mathcal{L}_{B-L} = -y_N \Phi \overline{(\nu_R)^c} \nu_R. \quad (38)$$

The scalar potential at tree-level is written as

$$V_{tree}(H, \Phi) = m_H^2 |H|^2 + m_S^2 |S|^2 + \lambda_H |H|^4 + \lambda_\Phi |\Phi|^4 + \lambda_{H\Phi} |H|^2 |\Phi|^2 \quad (39)$$

where H denotes the SM Higgs field. As noted in Ref. [4], all of the above Higgs potential parameters, consistent with the recent SM Higgs data [5], can be generated radiatively assuming a vanishing initial condition at a certain high scale Λ_{UV} . All the scales are generated by dimensional transmutation of the CW mechanism applied to the $B-L$ gauge symmetry breaking. In this setup, there are two free parameters, the extra gauge coupling g_X and the right-handed neutrino Yukawa coupling y_N , from which the $B-L$ breaking scale v_ϕ as well as the $B-L$ Higgs quartic coupling λ_Φ are generated dynamically. Extending the analysis of Ref. [4] to

higher v_ϕ scale, we will examine whether there exists an appropriate CW minimization point which is consistent with the observed cosmological quantities derived in the previous section.

Let us now consider the one-loop Coleman–Weinberg potential [2] for the $B-L$ sector. Taking $\Phi = \phi/\sqrt{2}$ in the unitary gauge and the normalization condition of $V''(0) = 0$ and $V''(Q) = 6\lambda_\Phi$, the one-loop corrected $B-L$ potential is given by [2]

$$V_X(\phi) = \frac{1}{4} \lambda_\Phi \phi^4 + \frac{1}{64\pi^2} \phi^4 (10\lambda_\Phi^2 + 48g_X^4 - 8y_N^4) \times \left(\ln \frac{\phi^2}{Q^2} - \frac{25}{6} \right) + V_0 \quad (40)$$

where we took one Yukawa coupling for the right-handed neutrinos y_N , and added a constant term V_0 normalizing the potential: $V_X = 0$ at the global minimum. Taking the renormalization scale at $Q = \langle \phi \rangle \equiv v_\phi$ to avoid the large-log uncertainty in the one-loop approximation [2], one can evaluate the minimization condition of the potential (40) and obtain

$$\lambda_\Phi(v_\phi) = \frac{11}{48\pi^2} (10\lambda_\Phi^2 + 48g_X^4 - 8y_N^4)(v_\phi). \quad (41)$$

This relation fixes the $B-L$ breaking scale v_ϕ in terms of input values of λ_Φ , g_X and y_N which evolve from the high scale Λ to v_ϕ by renormalization group. Putting back (41) into (40), one has

$$V_X(\phi) = \frac{3\lambda_\Phi}{22} \phi^4 \left(\ln \left(\frac{\phi}{v_\phi} \right) - \frac{1}{4} \right) + \frac{3\lambda_\Phi}{88} v_\phi^4, \quad (42)$$

which is nothing but the general CW potential given in Eq. (2) with $\lambda_\Phi \equiv 22A/3$.

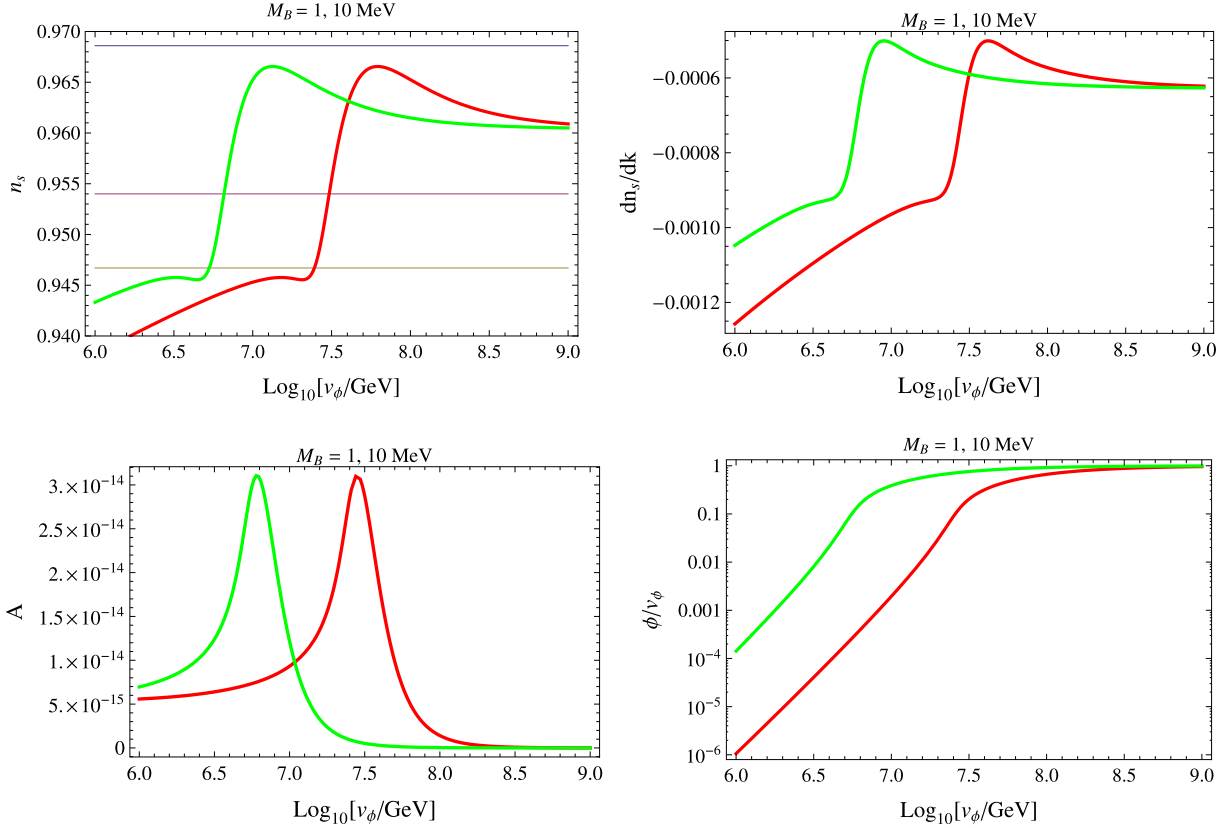


Fig. 6. The spectral index n_s , its running dn_s/dk , the quartic coupling A and the horizon-exit field value of ϕ/v_ϕ are shown in terms of the symmetry breaking scale v_ϕ for fixed brane scales $M_B = 1$ MeV (left green curve) and 10 MeV (right red curve) in each panel. The upper two horizontal lines in the first panel show n_s within the 1σ range of the Planck data and the lower line is the 2σ limit. (For interpretation of the references to color in this figure legend, the reader is referred to the web version of this Letter.)

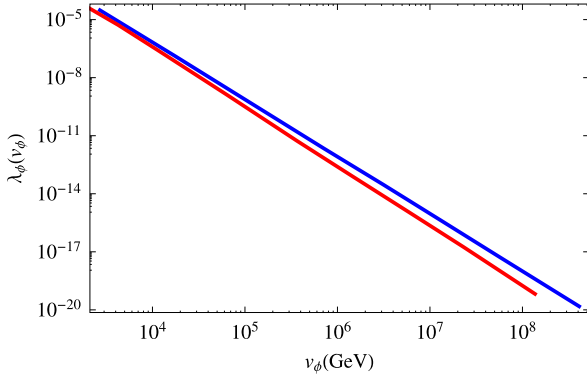


Fig. 7. The values of v_ϕ vs. λ_ϕ satisfying the CW minimization condition [4]. The upper (blue), and lower (red) lines correspond to the UV scale $M_X = 2 \times 10^{11}$ GeV, and 10^{18} GeV, respectively. (For interpretation of the references to color in this figure legend, the reader is referred to the web version of this Letter.)

In Fig. 7 we present the values of v_ϕ and λ_ϕ satisfying the CW minimization condition as well as the correct electroweak symmetry breaking for appropriate values of g_X . As noted in Ref. [4], one can see that larger v_ϕ requires smaller g_X . From Fig. 6, one can see that the spectral index n_s falls into the 1σ range of the Planck data for $v_\phi \gtrsim 5 \times 10^6$ GeV which requires $\lambda_\phi \approx 22A/3 \lesssim 2 \times 10^{-13}$. Furthermore, the required values of λ_ϕ drop rapidly for higher v_ϕ . Thus one finds viable parameter points around $v_\phi \sim 10^8$ GeV and $M_B \sim 1$ MeV in which the inflaton and Higgs potentials are generated simultaneously purely from radiative corrections. However, we should remark that the solutions to the minimization condition, $\lambda_\phi \sim 11/\pi^2 (g_X^4 - y_N^4/6)$, are found for fine-tuned choices

of $g_X^4 \simeq y_N^4/6$ resulting in highly suppressed values of λ_ϕ . It is expected that much less fine-tuned solutions would be found in some other $U(1)'$ models which have different beta-function coefficients.

5. Conclusions

We have analyzed the plausibility of a (small field) CW potential naturally arising from quantum corrections to address inflation in and beyond the standard cosmological scenario. We have shown that although it is not possible in the standard scenario to solve the horizon problem within 1σ consistency with the Planck measurement of the spectral index, brane-world scenarios ease the requirements on the numbers of e-folding needed to solve the horizon problem, while preserving the correlations among the other observables, allowing CW potentials to fulfill all the inflation requirements and remain an attractive and natural explanation for inflation. Besides, CW potentials have an inherent prediction on the relation between the running of the spectral index and the spectral index itself, which can be tested in the near future. Tensor modes are essentially absent in CW inflation models and thus, if found by next generation experiments, can rule out CW motivated inflationary potentials altogether.

The inflation observables can easily accommodate a rather small symmetry breaking scale $\sim 10^8$ GeV but do require a tiny quartic coupling $\sim 10^{-18}$. While the CW mechanism generates small scales through dimensional transmutation, such a tiny coupling may be indicative of a radiative origin. We have illustrated how dynamical generation of the inflaton as well as the SM Higgs potential can work consistently with the Planck results as well as the Higgs mass measurement at the LHC in the context of the SM

extended with the generalized $B - L$ gauge symmetry to explain the neutrino masses and mixing.

Acknowledgements

G.B. wishes to warmly thank KIAS Physics Group for its hospitality. She acknowledges support from the MEC and FEDER (EC) Grant FPA2011-23596 and the Generalitat Valenciana under Grant PROMETEOII/2013/017. H.M.L. was supported in part by Basic Science Research Program through the National Research Foundation of Korea (NRF) funded by the Ministry of Education, Science and Technology (2013R1A1A2007919). E.J.C. was supported by SRC program of NRF Grant No. 2009-0083526 funded by the Korea Government (MSIP) through Korea Neutrino Research Center.

References

- [1] P.A.R. Ade, et al., Planck Collaboration, arXiv:1303.5076; P.A.R. Ade, et al., Planck Collaboration, arXiv:1303.5082 [astro-ph.CO].
- [2] S.R. Coleman, E.J. Weinberg, Phys. Rev. D 7 (1973) 1888.
- [3] A.D. Linde, Phys. Lett. B 108 (1982) 389; A. Albrecht, P.J. Steinhardt, Phys. Rev. Lett. 48 (1982) 1220; R. Langbein, K. Langfeld, H. Reinhardt, L. von Smekal, Mod. Phys. Lett. A 11 (1996) 631–646, arXiv:hep-ph/9310335; P. Gonzalez-Diaz, Phys. Lett. B 176 (1986) 29; J. Yokoyama, Phys. Rev. D 59 (1999) 107303; M.U. Rehman, Q. Shafi, J.R. Wickman, Phys. Rev. D 78 (2008) 123516, arXiv:0810.3625.
- [4] E.J. Chun, S. Jung, H.M. Lee, Phys. Lett. B 725 (2013) 158, arXiv:1304.5815 [hep-ph]; Corrigendum in Phys. Lett. B and arXiv:1304.5815v3 [hep-ph].
- [5] G. Aad, et al., ATLAS Collaboration, Phys. Lett. B 716 (2012) 1, arXiv:1207.7214 [hep-ex]; S. Chatrchyan, et al., CMS Collaboration, Phys. Lett. B 716 (2012) 30, arXiv:1207.7235 [hep-ex].
- [6] R. Maartens, D. Wands, B.A. Bassett, I. Heard, Phys. Rev. D 62 (2000) 041301, arXiv:hep-ph/9912464.
- [7] L. Randall, R. Sundrum, Phys. Rev. Lett. 83 (1999) 4690, arXiv:hep-th/9906064; L. Randall, R. Sundrum, Phys. Rev. Lett. 83 (1999) 3370, arXiv:hep-ph/9905221.
- [8] J. Martin, C. Ringeval, V. Vennin, arXiv:1303.3787 [astro-ph.CO].
- [9] W.D. Goldberger, M.B. Wise, Phys. Rev. Lett. 83 (1999) 4922, arXiv:hep-ph/9907447.